



Optimizing the linear electron transport rate measured by chlorophyll a fluorescence to empirically match the gross rate of oxygen evolution in white light: Towards improved estimation of the cyclic electron flux around Photosystem I in leaves

Journal:	<i>Functional Plant Biology</i>
Manuscript ID	FP18039.R1
Manuscript Type:	Research paper
Date Submitted by the Author:	n/a
Complete List of Authors:	Zhang, Meng-Meng; Northeast Forestry University, Harbin, College of Life Science Fan, Da-Yong; Australian National University, Research School of Biology Sun, Guang-Yu; Northeast Forestry University, Harbin, College of Life Science Chow, Wah Soon; Australian National University, Research School of Biology
Keyword:	Chlorophyll fluorescence, Electron transport, Photosystem I, Photosystem II, Bioenergetics, Light reactions

SCHOLARONE™
Manuscripts

1

2 **Optimizing the linear electron transport rate measured by chlorophyll *a***
3 **fluorescence to empirically match the gross rate of oxygen evolution in white**
4 **light: Towards improved estimation of the cyclic electron flux around**
5 **Photosystem I in leaves**

6

7 Meng-Meng Zhang^{A,B}, Da-Yong Fan^B, Guang-Yu Sun^{A,C} and Wah Soon Chow^{B,C}

8 ^ACollege of Life Science, Northeast Forestry University, Harbin, Heilongjiang,
9 150040, China.

10 ^BDivision of Plant Sciences, Research School of Biology, The Australian National
11 University, Acton, ACT 2601, Australia.

12 ^CCorresponding author. E-mail: Fred.Chow@anu.edu.au; sungy@vip.sina.com

13

14

15 **Running title:** Optimizing matching of fluorescence- and O₂-based electron transport
16 rates

17

18 **Abbreviations:** AA, antimycin A; CEF, cyclic electron flux around PS I; Chl,
19 chlorophyll; ΔFlux , difference between ETR1 and ETR2 as an estimate of CEF;
20 ETR1, the electron flux through PS I; ETR2, the electron flux through PS II (and PS I
21 in series) measured as either LEF_n or LEF_{O_2} ; f_I , and f_{II} , the fraction of absorbed light
22 partitioned to PS I and PS II, respectively; F_m and F_m' , the maximum Chl fluorescence
23 yield in a dark-adapted state and a light-adapted state, respectively; F_s and F_o' , the
24 steady-state and minimum Chl fluorescence yield in a light-adapted state, respectively;
25 I , irradiance; LEF_n , the linear electron flux through both photosystems, measured by
26 chlorophyll fluorescence; LEF_{O_2} , the linear electron flux through both photosystems,
27 measured by the gross rate of oxygen evolution; MV, methyl viologen; NDH,
28 nicotinamide adenine dinucleotide dehydrogenase-like complex; P700, the special Chl
29 pair acting as the primary electron donor in PSI; PGR5, proton gradient regulation 5
30 protein; P_m and P_m' , signal corresponding to the maximum extent of oxidizable P700
31 in weak far-red light and in actinic light, respectively; PS I and PS II, Photosystem I
32 and II, respectively; qP , the photochemical quenching parameter; $Y(I)$ and $Y(II)$, the
33 photochemical yield of PS I and PS II, respectively.

34 **Summary Text for the Table of Contents**

35 Cyclic electron flow around Photosystem I (CEF) was discovered in isolated
36 chloroplasts more than six decades ago, but its quantification has been elusive. We
37 devised a method capable of estimating CEF in intact leaves attached to a plant. The
38 method involves measurement of (1) the total electron flux through Photosystem I by

39 a near-infra-red signal, and (2) the linear electron flux through both photosystems in
40 series by optimizing conditions of excitation and detection of chlorophyll
41 fluorescence.

42 **Abstract**

43 The cyclic electron flux (CEF) around photosystem I (PSI) was discovered in isolated
44 chloroplasts more than six decades ago, but its quantification has been hampered by
45 the absence of net formation of a product or net consumption of a substrate. We
46 estimated *in vivo* CEF in leaves as the difference (ΔFlux) between the total electron
47 flux through PSI (ETR1) measured by a near infra-red signal, and the linear electron
48 flux through both photosystems by optimized measurement of chlorophyll *a*
49 fluorescence (LEF_{fl}). Chlorophyll fluorescence was excited by modulated green
50 light from a light-emitting diode at an optimal average irradiance, and the
51 fluorescence was detected at wavelengths >710 nm. In this way, LEF_{fl} matched the
52 gross rate of oxygen evolution multiplied by 4 (LEF_{O_2}) in broad-spectrum white
53 actinic irradiance up to half (spinach, poplar and rice) or one-third (cotton) of full
54 sunlight irradiance. This technique of estimating CEF can be applied to leaves
55 attached a plant.

56 **Introduction**

57 Although discovered six decades ago (Arnon *et al.* 1955, Shikanai 2007), the cyclic
58 electron flux around Photosystem I (PSI) is difficult to quantify because there is
59 neither net formation of a product nor net consumption of a substrate. Currently, a

60 reasonable estimation involves measuring the total electron flux through PSI (ETR1)
61 and the linear electron flux through both photosystems in series under identical
62 illumination and sampling conditions. That is, ETR1 is measured by the redox
63 signal of P700, the primary electron donor in PSI in the form of a chlorophyll (Chl)
64 dimer in leaves. To obtain ETR1, the photochemical yield of PSI, $Y(I)$, given by the
65 fraction of P700 that can potentially be photo-oxidized under a given set of
66 measurement conditions (Klughammer and Schreiber 1994, 2007), was first
67 determined; $Y(I)$ can then be used to calculate ETR1 by taking into account the
68 irradiance, leaf absorbance and the fraction of absorbed light partitioned to PSI (f_I),
69 as well as assuming the quantum efficiency of photochemical conversion to be 1.0.
70 The linear electron flux through PSII and PSI in series (ETR2) was measured by the
71 gross rate of oxygen evolution using a Clarke-type oxygen electrode in CO₂-enriched
72 air in which photorespiration is suppressed (LEF_{O₂}). Both ETR1 and LEF_{O₂} are
73 measurements representative of the whole leaf tissue: oxygen is evolved from PSII
74 complexes that absorb light anywhere within the tissue, while the measuring beam for
75 detecting the P700⁺ signal (820 nm, with reference wavelength 870 nm), being only
76 weakly absorbed by P700⁺ and hardly absorbed by neutral chlorophyll (Chl)
77 molecules, is scattered repeatedly in the whole tissue until it is absorbed by P700⁺
78 (Oguchi *et al.* 2011).

79 The difference $ETR1 - LEF_{O_2} = \Delta Flux$ is approximately the cyclic electron
80 flux (CEF) if photorespiration and the local electron cycle in PSI in the form of
81 charge recombination are negligible. Alternatively, if oxygen evolution is assayed

82 by membrane-inlet mass spectrometry, the oxygen uptake in photorespiratory
83 conditions can be taken into account; the method can then be used in ambient air
84 (although the draw-down of CO₂ in a closed chamber rapidly changes the [CO₂] in
85 ambient air), provided charge recombination in PSI is negligible. However,
86 membrane-inlet mass spectrometry is not as readily available as a Clarke-type oxygen
87 electrode.

88 Another disadvantage associated with oxygen measurement is that a leaf
89 segment is cut and placed in a chamber, either that of an oxygen electrode or that of a
90 mass spectrometer, making *in situ* measurement of leaves attached to a plant
91 impossible. A further disadvantage is that, since oxygen measurements are generally
92 slow, there is limited time resolution to monitor the time course of CEF, for example,
93 during photosynthetic induction. Thus, assaying linear electron flux by oxygen
94 measurement can present a number of shortcomings (Fan *et al.* 2016).

95 The linear electron flux (ETR₂) through both photosystems can also be measured
96 by Chl *a* fluorescenc, which yields the photochemical yield of PSII, Y(II). Y(II) can
97 then be used to calculate ETR₂ (specifically termed LEF_{II} here) by taking into account
98 the irradiance, leaf absorptance and f_{II} the fraction of absorbed light partitioned to
99 PSII (Genty *et al.* 1989; Evans *et al.* 2017). Chl fluorescence can be measured on a
100 leaf attached to a plant, in photorespiratory conditions and with good time resolution.
101 Unfortunately, without optimizing the conditions of Chl fluorescence measurement,
102 ETR₂ so obtained can be considerably less than LEF_{O₂} in broad-spectrum white

103 actinic light, when the modulated measuring (excitation) light is blue (Kou *et al.*
104 2013). This underestimation of the linear electron flux is due to the inherently
105 localized detection of the Chl fluorescence signal from a shallow depth of the leaf
106 tissue (Oguchi *et al.* 2011). Under other conditions, where the *actinic* light is blue
107 but the modulated measuring light is red, Chl fluorescence-based ETR2 can be
108 considerably *greater* than the linear electron transport rate obtained from the gross
109 rate of CO₂ assimilation (Evans *et al.* 2017); this observation can be explained by a
110 multilayer photosynthesis model (Evans 2009; Evans *et al.* 2017). The aim of this
111 present study is to select conditions in which LEF_{fl} is more representative of the
112 whole tissue, so that it can match LEF_{O2}, both measured in broad-spectrum white light;
113 LEF_{fl} can then be subtracted from ETR1 to yield a reasonable estimate of CEF. This
114 method allows us to estimate CEF in leaves attached to a plant even in
115 photorespiratory conditions, at least up to a certain actinic irradiance, as demonstrated
116 in four plant species.

117 **Materials and methods**

118 **Plant growth**

119 Four plant species, *Spinacia oleracea* L. (cv. Yates hybrid 102), *Populus canadensis*
120 cv. 'Evergreen 65-1', *Oryza sativa* L. (spp. Japonica) and *Gossypium hirsutum* L. (cv.
121 Sicot 75), were grown in a glasshouse (~30/15 °C, day/night); they represent,
122 *respectively*, various plant types: herbaceous, woody, monocot, and *a perennial plant*
123 *that is usually grown as an annual crop*. A nutrient mix (Aquasol, Hortico, Clayton,

124 Australia) was supplemented by a slow release fertilizer ('Osmocote', Scotts Australia
125 Pty Ltd, Castle Hill). Young fully-expanded leaves were used for measurements.

126 **Measurements of O₂ evolution**

127 O₂ evolution from leaf discs was measured in a gas-phase oxygen electrode
128 (Hansatech, King's Lynn, UK) chamber maintained at 25°C. The sample chamber
129 contained 1% CO₂ supplied by fabric matting moistened with 1 M NaHCO₃/Na₂CO₃
130 (pH = 9). O₂ evolution was measured in continuous white light from a halogen lamp
131 (400-740 nm, peak spectral irradiance 620 nm, with about 7% of the irradiance within
132 the wavelength range 700-740 nm) over several minutes until steady state. The
133 slope at approximately 40 s after cessation of illumination (when a cooling artefact
134 had subsided) was subtracted algebraically from the steady-state net oxygen evolution
135 rate to yield the *gross* oxygen evolution rate. The gross oxygen evolution rate was
136 multiplied by 4 to obtain the linear electron flux LEF_{O₂}. The actinic irradiance was
137 varied by increasing it in steps from darkness to yield a light-response curve. For
138 calibration of the oxygen signals, 1 mL of air at 25°C (taken to contain 8.05 μmol O₂)
139 was injected into the gas-phase O₂ electrode chamber.

140 **Measurement of Chl *a* fluorescence**

141 A pulse amplitude modulation fluorometer PAM 101/103 (Walz, Effeltrich, Germany)
142 was used to measure Y(II). The modulated excitation light (1.6 kHz, unless
143 automatically switched to 100 kHz when the saturating pulse was applied) was either

144 blue (wavelength 462 nm, average irradiance = $0.05 \mu\text{mol m}^{-2} \text{s}^{-1}$), red (wavelength
145 665 nm, $0.05 \mu\text{mol m}^{-2} \text{s}^{-1}$) or green (wavelength 511 nm, up to $0.38 \mu\text{mol m}^{-2} \text{s}^{-1}$).
146 To obtain sufficient green excitation irradiance, several commercial green LEDs were
147 tested. The chosen green LED (Cree C503B-GAN 535 nm Green LED) was the
148 brightest, and was driven by an amplified (modulated) voltage from the Emitter
149 terminal of the PAM 101. A stainless-steel metal mesh, of the kind used in a
150 Hansatech oxygen electrode, was placed underneath a leaf disc or a leaf attached to a
151 plant, to reflect green excitation light back into the leaf tissue, while allowing gas
152 diffusion in and out of the abaxial side.

153 A saturating pulse of white light, of duration 0.8 s and irradiance $7,300 \mu\text{mol m}^{-2}$
154 s^{-1} , was used to obtain the maximum Chl fluorescence yield in a dark-adapted sample
155 (F_m) or a light-adapted sample (F_m'). In retrospective tests of saturation by the pulse
156 of white light, we compared LEF_{fl} obtained using a saturating pulse of irradiance
157 $12,000 \mu\text{mol m}^{-2} \text{s}^{-1}$ or $7,300 \mu\text{mol m}^{-2} \text{s}^{-1}$. The increases in LEF_{fl} (using an average
158 green excitation irradiance of $0.24 \mu\text{mol m}^{-2} \text{s}^{-1}$) that we obtained at $12,000 \mu\text{mol m}^{-2}$
159 s^{-1} compared with $7,300 \mu\text{mol m}^{-2} \text{s}^{-1}$ were at most (at the actinic irradiance $1,500 \mu\text{mol}$
160 $\text{m}^{-2} \text{s}^{-1}$) only slight for spinach (2%), poplar (4%), rice (4%) and cotton (5%). Below
161 $1,000 \mu\text{mol m}^{-2} \text{s}^{-1}$, (spinach, poplar and rice) or $600 \mu\text{mol m}^{-2} \text{s}^{-1}$ (cotton), there was
162 no statistical difference between $12,000 \mu\text{mol m}^{-2} \text{s}^{-1}$ $7,300 \mu\text{mol m}^{-2} \text{s}^{-1}$. Thus, we
163 consider a pulse at $7,300 \mu\text{mol m}^{-2} \text{s}^{-1}$ to be saturating for the actinic irradiance range
164 relevant to this study.

165 The Chl fluorescence was measured via the Detector terminal of the PAM 101
166 (Walz, Effeltrich, Germany), using a filter which transmitted fluorescence of
167 wavelength >710 nm. The rationale of selecting longer wavelengths is the
168 expectation that re-absorption of long-wavelength fluorescence would be minimized,
169 thereby allowing detection from greater depths in the tissue.

170 The photochemical yield of PSII, $Y(II)$, was calculated as $1 - F_s/F_m'$, where F_s is
171 the steady-state fluorescence yield and F_m' the maximum fluorescence yield in the
172 light-adapted state (Genty *et al.* 1989). The fluorescence-based linear rate of
173 electron transport through PSII (and PSI) was calculated as $LEF_{II} = Y(II) \times I \times 0.85 \times$
174 0.5 , where I is the irradiance, 0.85 the leaf absorptance and 0.5 the assumed
175 partitioning (also see experimental estimations in Table 1) of the absorbed light
176 between the two photosystems.

177 The photochemical quenching parameter qP was calculated as $(F_m' - F_s)/(F_m' -$
178 $F_o')$, where F_o' is the minimum Chl fluorescence yield of open PSII reaction centre
179 traps in the light-adapted state. F_o' was calculated according to Oxborough and
180 Baker (1997).

181 **Measurement of the P700⁺ signal from leaf segments**

182 Measurement of the photochemical yield of PSI, $Y(I)$, is based on the technique of
183 Klughammer and Schreiber (1994, 2007), slightly modified by introducing a strong
184 far-red pulse shortly before the saturating pulse of white light, as described by Kou *et*
185 *al.* (2013). The measurement employed a dual-wavelength (820/870 nm) P700 unit

186 (ED-P700DW) connected to a pulse amplitude modulation (PAM 101) fluorometer
187 (Walz, Effeltrich, Germany) in the reflectance mode, with a metal mesh underneath
188 the abaxial side of a leaf segment inside a gas-phase oxygen electrode in which the
189 upper water jacket had a vertical port for accepting a multifurcated light guide.
190 When a leaf attached to the plant was sampled, the same upper water jacket was
191 placed on the leaf, with the metal mesh underneath the leaf. The metal mesh served
192 to reflect the near-infra-red measuring beam or the fluorescence excitation light back
193 to the leaf tissue, while allowing gas diffusion into the abaxial side of the leaf.
194 Actinic illumination was provided to the adaxial side of the leaf disc. Timing of data
195 acquisition and application of various lights was controlled by a pulse-delay generator
196 (Model 555, Berkeley Nucleonics, San Rafael, CA, USA).

197 The measurement of $Y(I)$ was conducted in two stages (Kou *et al.* 2013). First,
198 a leaf sample was illuminated to steady state for about 10 minutes during which
199 oxygen evolution or Chl fluorescence was monitored. Then the system was quickly
200 (within < 1 min during which the leaf sample was in darkness) switched to P700⁺
201 measurement. To re-establish steady state, the leaf sample was illuminated with a
202 given actinic light for 8.8 s before data acquisition started, followed by a strong
203 far-red pulse ($600 \mu\text{mol m}^{-2} \text{s}^{-1}$, 100 ms duration), in the middle of which a saturating
204 pulse ($10,000 \mu\text{mol m}^{-2} \text{s}^{-1}$, 10 ms duration) was applied to reach the maximum
205 permissible oxidation of P700 (P_m') in the presence of actinic light. The duration of
206 total actinic illumination was 9.0 s. The sequence was repeated every 9.3 s, so that
207 the dark time (which helped to establish the baseline corresponding to fully reduced

208 P700) between repeats was about 3.2% of the total length of time. Twenty-five
209 repeat signals were averaged.

210 The second stage of Y(I) measurement was to determine the maximum signal
211 corresponding the maximum P700 photo-oxidation when the acceptor-side limitation
212 was negligible. Weak far-red light ($92 \mu\text{mol m}^{-2} \text{s}^{-1}$) was applied to attain a steady
213 P700⁺ concentration. Then a saturating pulse (0.5 ms duration, $10,000 \mu\text{mol m}^{-2} \text{s}^{-1}$)
214 was applied to fully oxidize the remaining P700 (P_m). The values of P_m , P_m' , and the
215 steady-state oxidation state of P700 in the presence of a given actinic light were used
216 to calculate Y(I) according to Klughammer and Schreiber (2007).

217 Results

218 Light-response curves of photosynthetic electron transport determined via gross 219 oxygen evolution and via the yield of Chl *a* fluorescence excited by blue, red or 220 green modulated light

221 The gross rate of oxygen evolution, in white halogen light and in 1% CO₂, of spinach
222 leaf discs cut from plants grown in a glasshouse showed typical responses. At the
223 maximum irradiance of almost $1,700 \mu\text{mol m}^{-2} \text{s}^{-1}$ tested, the gross rate of oxygen
224 evolution multiplied by 4 (LEF_{O2}) was nearly, but not yet fully, light-saturated (Fig. 1,
225 closed circles). LEF_{O2} was compared with the fluorescence-based LEF_{fl}. Fig. 1
226 shows that the extent of matching of LEF_{fl} with LEF_{O2} varied with irradiance and with
227 wavelength of the modulated excitation light. At low actinic irradiance, below about

228 $500 \mu\text{mol m}^{-2} \text{s}^{-1}$, the matching was good regardless of excitation wavelength.
229 Above this irradiance, however, the matching was the poorest with blue, and then red
230 excitation light. Matching was improved with green excitation light; at an average
231 excitation irradiance of $0.38 \mu\text{mol m}^{-2} \text{s}^{-1}$, the matching was better than with 0.05
232 $\mu\text{mol m}^{-2} \text{s}^{-1}$. However, above actinic irradiance $1,100 \mu\text{mol m}^{-2} \text{s}^{-1}$, the
233 fluorescence-based LEF_{fl} underestimated the linear electron flux obtained as LEF_{O_2} .

234 Similarly, poplar leaf discs in 1% CO_2 showed poor matching of LEF_{O_2} and LEF_{fl}
235 obtained in blue excitation light, slightly better matching in red excitation light, and
236 somewhat better matching with weak green excitation light ($0.07 \mu\text{mol m}^{-2} \text{s}^{-1}$, Fig.
237 2a). In another batch of poplar plants, matching was good at an average green
238 excitation irradiance of $0.38 \mu\text{mol m}^{-2} \text{s}^{-1}$, up to an actinic irradiance of $\sim 1,000 \mu\text{mol}$
239 $\text{m}^{-2} \text{s}^{-1}$ (Fig. 2b). At even higher green excitation irradiance, the matching
240 deteriorated (data not shown).

241 In rice leaf segments measured in 1% CO_2 , the matching was similarly improved
242 as the green excitation light increased to $0.38 \mu\text{mol m}^{-2} \text{s}^{-1}$ (Fig. 3). However, when
243 the actinic irradiance exceeded $\sim 1,100 \mu\text{mol m}^{-2} \text{s}^{-1}$, the matching deteriorated, LEF_{fl}
244 being considerably smaller than LEF_{O_2} .

245 In cotton leaf discs measured in 1% CO_2 , the matching also improved as the
246 excitation light was changed from blue to red to green. However, the matching was
247 not good when the actinic irradiance exceeded $\sim 700 \mu\text{mol m}^{-2} \text{s}^{-1}$, even with green
248 excitation light. This maximum actinic irradiance for good matching is lower in

249 cotton than in the other three plant species.

250 **Estimation of cyclic electron flux around PSI as the difference (ΔFlux) between**
251 **ETR1 and LEF_{fl}**

252 Given the reasonably good matching between LEF_{fl} and LEF_{O_2} when Chl *a*
253 fluorescence was excited by green light at $0.38 \mu\text{mol m}^{-2} \text{s}^{-1}$ and in white actinic light
254 of irradiance $< 1,000 \mu\text{mol m}^{-2} \text{s}^{-1}$ (spinach, poplar and rice leaves), or $< 700 \mu\text{mol}$
255 $\text{m}^{-2} \text{s}^{-1}$ (cotton leaves), we proceeded to estimate cyclic electron flux around PSI as
256 the difference (ΔFlux) between ETR1 and LEF_{fl} . These electron fluxes were
257 determined on intact leaves attached to the plant in air, or in leaf discs in air enriched
258 with 1% CO_2 , the latter conditions used in oxygen measurements. In spinach leaves
259 attached to the plant in air, LEF_{fl} was not yet saturated at $1,100 \mu\text{mol m}^{-2} \text{s}^{-1}$, and
260 ETR1 was even less light-saturated (Fig. 5a). ΔFlux , was very small (relative to
261 LEF_{fl}) at irradiance $< 300 \mu\text{mol m}^{-2} \text{s}^{-1}$; above $500 \mu\text{mol m}^{-2} \text{s}^{-1}$, however, it increased
262 steadily until, at $1,000 \mu\text{mol m}^{-2} \text{s}^{-1}$, it was about one-third of LEF_{fl} . Similar results
263 for ΔFlux were obtained with spinach leaf discs in 1% CO_2 (Fig. 5b).

264 Spinach leaf discs were vacuum infiltrated with water (control), $200 \mu\text{M}$
265 antimycin A (AA, an inhibitor of the PGR5-dependent cyclic pathway) or $100 \mu\text{M}$
266 methyl viologen (MV, a mediator of electron transfer to molecular oxygen). Excess
267 intercellular water was allowed to evaporate in darkness until the tissue was no longer
268 translucent, before measurements. Table 2 shows that ΔFlux was close to zero after
269 these treatments.

270 In an intact poplar leaf attached to a cut branch of a plant, ΔFlux was very small
271 (relative to LEF_{fl}) in white actinic light below actinic irradiance $100 \mu\text{mol m}^{-2} \text{s}^{-1}$,
272 above which it increased practically linearly (Fig. 6a). In cut leaf discs in 1% CO_2 ,
273 ΔFlux increased in the same way as in the intact leaf, even though ETR1 was
274 somewhat smaller at high actinic irradiance, and LEF_{fl} showed a slight decline at high
275 actinic irradiance (Fig. 6b).

276 In rice leaves attached to the plant, ΔFlux was negligibly small (relative to LEF_{fl})
277 below actinic irradiance $200 \mu\text{mol m}^{-2} \text{s}^{-1}$. It then increased linearly up to the
278 maximum actinic irradiance $1,100 \mu\text{mol m}^{-2} \text{s}^{-1}$, at which it reached 62% of LEF_{fl}
279 (Fig. 7a). In cut rice leaf segments in 1% CO_2 (Fig. 7b), both ETR1 and LEF_{fl} were
280 smaller than in intact leaves. Nonetheless, ΔFlux behaved similarly as in intact
281 leaves.

282 In cotton leaves, we had to restrict the actinic irradiance to below $800 \mu\text{mol m}^{-2}$
283 s^{-1} for matching of LEF_{O_2} and LEF_{fl} . The LEF_{fl} so obtained was similar in an intact
284 leaf attached to the plant in air to that of a leaf disc in 1% CO_2 (Fig. 8). In either
285 case, ΔFlux (relative to LEF_{fl}) was negligibly small below $100 \mu\text{mol m}^{-2} \text{s}^{-1}$, but it
286 increased linearly above that irradiance. ΔFlux was slightly larger in an intact cotton
287 leaf than in a cut leaf disc.

288 **The decrease in LEF_{fl} at high actinic irradiance**

289 At high actinic irradiance, LEF_{fl} decreased in all four species, resulting in a deviation

290 from the LEF_{O_2} curve. To investigate the reason behind the decrease in LEF_{fl} , we
291 plotted $qP \times I$ (the product of the photochemical quenching parameter and irradiance)
292 against irradiance (Fig. 9a) in cotton leaves. It is seen that $qP \times I$ increased rapidly
293 with irradiance, then more slowly and even decreased slightly at irradiance >700
294 $\mu\text{mol m}^{-2} \text{s}^{-1}$, implying that qP decreased more drastically than irradiance increased.
295 By contrast, a plot of $(F_v'/F_m') \times I$ (the product of the light-adapted ratio of variable
296 fluorescence to maximum fluorescence and irradiance) against irradiance is a nearly
297 straight line, implying that F_v'/F_m' was relatively constant.

298 DISCUSSION

299 One method of estimation of CEF involves determination of both the electron flux
300 through PSI (ETR1) and the linear electron flux (LEF_{O_2}) through both photosystems
301 in series under identical conditions (Kou *et al.* 2013). Determination of LEF_{O_2} in an
302 oxygen electrode necessitates the use of a high CO_2 concentration to suppress
303 photorespiration and the cutting of a leaf segment or disc to be placed in the electrode
304 chamber. Further, oxygen measurements are inherently slow and, therefore, unable
305 to follow changes in CEF with sufficient time resolution, for example, during
306 photosynthetic induction. These shortcomings prompted us to seek an alternative
307 method of determining the linear electron flux.

308 Chlorophyll *a* fluorescence potentially offers such a convenient and
309 non-intrusive technique: it can be applied to an intact leaf attached to a plant, in air,
310 and with good resolution time. Various studies have attempted to correlate Chl *a*

311 fluorescence parameters with gas-exchange measurements. For instance, Weis and
312 Berry (1987) obtained a linear plot of ϕ_{O_2}/qP against qN , where ϕ_{O_2} is the gross rate of
313 oxygen evolution divided by the irradiance I , qP is a photochemical quenching
314 parameter and qN is a non-photochemical quenching parameter. In principle,
315 measurements of qP , qN and I should yield the gross rate of oxygen evolution from an
316 equation fitted to the linear plot. Unfortunately, the relationship is not universal
317 among leaves of plants; there are occasional exceptions to a single straight line
318 (Öquist and Chow 1992).

319 Genty *et al.* (1987) reported a near-linear relation between $Y(II)$ and ϕ_{CO_2} , the
320 CO_2 assimilation rate per unit irradiance in barley and maize, as did Edwards and
321 Baker (1993) in maize. Seaton and Walker (1990) and Öquist and Chow (1992), on
322 the other hand, observed a curvilinear relation between $Y(II)$ and ϕ_{O_2} , the gross O_2
323 evolution rate per unit irradiance. Further, there were exceptions to what appeared at
324 first sight to be a universal relation that can be fitted by a single curve (Öquist and
325 Chow 1992). The difficulty of obtaining a universal relation between Chl
326 fluorescence measurements and gas-exchange measurements is no doubt due to the
327 differential sampling of the leaf tissue by the two techniques: oxygen is evolved from
328 the whole tissue, but the fluorescence is predominantly detected from chloroplasts
329 near the surface of the leaf facing the detector. For this reason, fluorescence-derived
330 LEF_{fl} depends on the spectral quality of the measuring beam, that of the actinic light,
331 and the wavelength band over which the fluorescence is detected (Evans *et al.* 2017).
332 By attempting to optimize the fluorescence measurement in this study, we hoped to

333 obtain a signal that is more representative of the whole leaf tissue and, therefore,
334 better matched with gas exchange measurements, at least up to a certain actinic
335 irradiance.

336 **Optimizing LEF_{fl} to match LEF_{O_2}**

337 We used green excitation light which is attenuated more slowly as it penetrates the
338 leaf tissue (Terashima *et al.* 2009) and which, therefore, reports from greater depths in
339 the leaf tissue. We also detected Chl fluorescence at wavelengths ≥ 710 nm; the
340 long-wavelength emission, if occurring from deep tissue, is less likely to be
341 re-absorbed by chlorophyll on its way to the detector. Using these measurement
342 conditions, we obtained $LEF_{fl} = Y(II) \times I \times 0.85 \times 0.5$, as explained in Methods. The
343 assumed partitioning of the absorbed, broad-spectrum halogen light between the two
344 photosystems is 0.5 to each photosystem. For spinach grown in a glasshouse, this
345 was indeed the case experimentally (Fan *et al.* 2016). Below, we experimentally
346 obtain the partitioning of broad-spectrum halogen light for the four species, all grown
347 in the same glasshouse. It is noted that at low actinic irradiance (≤ 500 for spinach
348 and rice; $\leq 150 \mu\text{mol m}^{-2} \text{s}^{-1}$ for cotton and poplar), the variation of LEF_{fl} with actinic
349 irradiance was practically independent of the spectral quality and/or irradiance of the
350 weak excitation light. This is probably because, at a relatively low actinic irradiance,
351 only the chloroplasts in shallow leaf tissue were photosynthesizing to any great extent.
352 Under such conditions, by simply equating $Y(II) \times I \times 0.85 \times f_{II}$ with LEF_{O_2} for
353 irradiance $\leq 150 \mu\text{mol m}^{-2} \text{s}^{-1}$ (poplar and cotton) or $\leq 500 \mu\text{mol m}^{-2} \text{s}^{-1}$ (spinach and

354 rice), we derived values of f_{II} as shown in Table 1. The average f_{II} is very close to
355 0.5, justifying our use of the value of $f_{II} = 0.5$ for the partitioning to PSII and $f_I = 0.5$
356 for the partitioning to PSI in the four species, in broad-spectrum white light.

357 The linear electron flux detected by Chl fluorescence LEF_{F_0} flows through both
358 photosystems in series, to reduce $NADP^+$ to NADPH or, to a much lesser extent in
359 angiosperms, reduce O_2 to form superoxide in the Mehler reaction. The linear
360 electron flux detected as oxygen evolution LEF_{O_2} , on the other hand, would be
361 underestimated if oxygen were simply consumed in the Mehler reaction. However,
362 the resulting superoxide is scavenged in the water-water cycle to release oxygen again
363 (Asada 2000, Miyake 2010); therefore, no net consumption of oxygen occurs despite
364 any Mehler reaction, and LEF_{O_2} correctly measures the linear electron flux through
365 both photosystems even when the Mehler reaction occurs, provided the water-water
366 cycle runs efficiently. Thus, neither LEF_{F_0} nor LEF_{O_2} is compromised by any Mehler
367 reaction.

368 At high actinic irradiance it is obvious that, to obtain good matching between
369 LEF_{F_0} and LEF_{O_2} , excitation with blue light was not as good as with red light, which
370 was not as good as with green light; further, a higher average excitation irradiance of
371 green light, up to about $0.38 \mu\text{mol m}^{-2} \text{s}^{-1}$, seemed to be optimal. (Figs. 1-4). Thus,
372 using this green optimal irradiance for the measuring beam, there was good matching
373 of LEF_{O_2} and LEF_{F_0} up to a broad-spectrum actinic irradiance of $\sim 1,000 \mu\text{mol m}^{-2} \text{s}^{-1}$
374 for spinach, rice and poplar, and about $700 \mu\text{mol m}^{-2} \text{s}^{-1}$ for cotton leaves.

375 Beyond the maximum actinic irradiance below which the matching was good,
376 LEF_{fl} decreased slightly, even when LEF_{O_2} continued to increase with irradiance.
377 This discrepancy between LEF_{fl} and LEF_{O_2} at high actinic irradiance prompted us to
378 re-measure LEF_{fl} using two saturating pulses, one at irradiance $12,000 \mu\text{mol m}^{-2} \text{s}^{-1}$,
379 and the other at $7,300 \mu\text{mol m}^{-2} \text{s}^{-1}$ which was originally used. The increases in LEF_{fl}
380 (using an average green excitation irradiance of $0.24 \mu\text{mol m}^{-2} \text{s}^{-1}$) that we obtained at
381 $12,000 \mu\text{mol m}^{-2} \text{s}^{-1}$ compared with $7,300 \mu\text{mol m}^{-2} \text{s}^{-1}$ were at most (at the actinic
382 irradiance $1,500 \mu\text{mol m}^{-2} \text{s}^{-1}$) only slight for spinach (2%), poplar (4%), rice (4%) and
383 cotton (5%) (Data not shown). These differences, while real, are not sufficient to
384 explain the discrepancy between LEF_{fl} and 4 x the gross oxygen evolution rate at
385 actinic irradiance $1,500 \mu\text{mol m}^{-2} \text{s}^{-1}$ (13% for spinach, 28% for poplar, 17% for rice
386 and 28% for cotton). In all four plant species, no significant difference in LEF_{fl}
387 between the two saturating pulse intensities was obtained when the actinic irradiance
388 was below a certain value: $1,000 \mu\text{mol m}^{-2} \text{s}^{-1}$ for spinach, rice and poplar, and 660
389 $\mu\text{mol m}^{-2} \text{s}^{-1}$ for cotton. That is, a pulse at $7,300 \mu\text{mol m}^{-2} \text{s}^{-1}$ was saturating at or
390 below these irradiances; these are also actinic irradiance values below which we
391 obtained a good empirical matching of LEF_{fl} and LEF_{O_2} .

392 The slight decrease in LEF_{fl} at high actinic irradiance is almost certainly due to
393 detection of the fluorescence predominantly from chloroplasts in shallower depths of
394 the tissue. In shallow tissue the actinic irradiance is not yet attenuated substantially,
395 and Q_A is in a more reduced state (qP lower) than is the case in deeper tissue.
396 Indeed, plotting the product of qP and I against I gave a curve that reached a

397 maximum at an irradiance at which LEF_{fl} began to deviate from LEF_{O_2} (Fig. 9a).
398 Above that maximum irradiance, $qP \times I$ even declined slightly with increase in
399 irradiance. Since $LEF_{\text{fl}} = Y(\text{II}) \times I \times 0.85 \times f_{\text{fl}}$, where $Y(\text{II}) = qP \times F_v'/F_m'$, there is
400 an underestimation of LEF_{fl} due to the use of a qP that represents chloroplasts in
401 shallower depths of the tissue rather than in the whole tissue. By contrast to qP , the
402 photochemical yield of open PSII reaction centre traps (F_v'/F_m') was rather constant,
403 since a plot of the product of F_v'/F_m' and I against I yielded a near-straight line (Fig.
404 9b).

405 **Estimation of CEF from the difference between ETR1 and LEF_{fl}**

406 Since Chl fluorescence can be measured from a leaf attached to a plant, and since
407 LEF_{fl} and LEF_{O_2} can be empirically matched, at least up to a certain maximum actinic
408 irradiance, we are in a position to estimate CEF as the difference between ETR1 and
409 LEF_{fl} in intact spinach leaves in air. Fig. 5a shows ETR1 increasing with irradiance,
410 even when LEF_{fl} began to plateau. The difference (ΔFlux) is attributable mainly to
411 CEF, since ΔFlux at $980 \mu\text{mol m}^{-2} \text{s}^{-1}$ in spinach leaf discs is almost completely
412 inhibited by antimycin A (Kou *et al.* 2013) and completely abolished by antimycin A
413 or MV as shown in Table 2. At $980 \mu\text{mol m}^{-2} \text{s}^{-1}$, ΔFlux (= ETR1 - LEF_{fl}) was
414 approximately one-third of LEF_{fl} in an intact spinach leaf (Fig. 5a), just as ΔFlux (in
415 that case the difference between ETR1 and LEF_{O_2}) was about one-third of LEF_{O_2} in
416 leaf discs in 1% CO_2 (Kou *et al.* 2013). Further, at actinic irradiance $<300 \mu\text{mol m}^{-2}$
417 s^{-1} , ΔFlux was very small relative to LEF_{fl} , just there was little ΔFlux at low actinic

418 irradiance when compared with LEF_{O_2} (Kou et al. 2013). There was little difference
419 between the $\Delta Flux$ of an intact spinach leaf in air in the laboratory environment and
420 that of leaf discs in 1% CO_2 .

421 $\Delta Flux$ in spinach leaf discs after vacuum infiltration with antimycin A (AA) was
422 close to zero at both 500 and 1,000 $\mu mol m^{-2} s^{-1}$ (Table 2). This suggests that AA
423 inhibited the PGR5-dependent CEF pathway completely. Further, this result
424 indicates that, in spinach, there was little or no charge recombination in PSI at these
425 irradiances, for any charge recombination would have contributed to a residual $\Delta Flux$.
426 In *Arabidopsis thaliana*, the NDH-dependent pathway is minor compared with the
427 PGR5-dependent CEF pathway and NDH may even aid the AA-sensitive,
428 PGR5-dependent CEF pathway (Kou et al. 2015). In the presence of MV, $\Delta Flux$ was
429 also close to zero. MV, by mediating electron transfer to molecular oxygen, should
430 have minimized both CEF and charge recombination, so this result was expected.
431 Unfortunately, we were not able to use vacuum infiltration on leaf tissues of the other
432 three species without losing photosynthetic activity. Uptake through the cut petioles
433 of poplar and cotton leaves overnight was attempted, as was floating leaf discs on
434 solutions, but we were not confident that the inhibitors were reaching all the intended
435 sites of action.

436 In intact poplar leaves attached to a branch (Fig. 6a) and in cotton leaves
437 attached to the plant (Fig. 8a), $\Delta Flux$ increased with actinic irradiance with a smaller
438 lag ($< 100 \mu mol m^{-2} s^{-1}$) than in the other two species. The same was true of leaf

439 discs in 1% CO₂ (Fig. 6b). The decrease in LEF_{fl} at high actinic irradiance was more
440 pronounced in leaf discs than in an intact leaf. This could be due to some water loss
441 which resulted in tissue contraction of leaf discs, thereby exacerbating the difficulty
442 of detecting the fluorescence from the chloroplasts in deeper tissue.

443 ETR1 was greater in intact rice leaves compared with leaf segments, as was
444 the case of LEF_{fl}. This observation confirms that measurements on intact leaves are
445 superior to those on leaf discs of some plant species, and justifies the search for a
446 method, such as Chl fluorescence in this study, that allows measurements on an intact
447 system. Possibly, linear electron transport in rice segments was decreased by
448 stomatal closure associated with water loss from the cut tissue (Fig. 7). In intact rice
449 leaves in air as well as leaf segments in 1% CO₂, a lag (up to ~200 μmol m⁻² s⁻¹) was
450 also apparent before ΔFlux increased steadily with irradiance (Fig. 7). At 1,000
451 μmol m⁻² s⁻¹, ΔFlux was comparable to LEF_{fl} in cut leaf segments, whereas it was
452 only about 60% of LEF_{fl} in intact leaves. This could be due to water loss from leaf
453 segments; water deficit increases CEF as estimated in various ways (Golding *et al.*
454 2004; Kohzuma *et al.* 2009; Kou *et al.* 2013), despite a decrease in linear electron
455 transport.

456 Cotton leaf discs showed matching of LEF_{O2} and LEF_{fl} up to a lower maximum
457 actinic irradiance than the other three species, so we measured ETR1 and LEF_{fl} only
458 up to 800 μmol m⁻² s⁻¹. Above ~100 μmol m⁻² s⁻¹, ΔFlux increased steadily in both
459 intact cotton leaves attached to the plant and in leaf discs in 1% CO₂, reaching ≥ 50%

460 of LEF_{fl} at the highest irradiance, $800 \mu\text{mol m}^{-2} \text{s}^{-1}$. Cyclic electron transport is a
461 significant contributor to (1) the resistance of cotton to high-light stress, facilitating
462 movement of cotton leaves to track the sun and intercept more radiation (Yao *et al.*
463 2018) and (2) improving the stability of the two photosystems under mild water
464 deficit conditions (Yi *et al.* 2018).

465 In summary, we selected conditions of measurement so that LEF_{fl} matched LEF_{O_2}
466 quite closely, but only up a certain maximum irradiance of actinic light supplied from
467 a halogen lamp. Up to this maximum actinic irradiance, it is possible to estimate
468 CEF as the difference (ΔFlux) between ETR1 and LEF_{fl} in leaves attached the plant.

469 **Acknowledgements**

470 The authors declare no conflicts of interest. This work was supported by a China
471 Scholarship Council Fellowship (to M-M Z), and a grant from the Australian
472 Research Council (to WSC, DP1093827). We thank Adam Pynt for modifying the
473 PAM 101 to enable excitation with green light. We are grateful to Reviewer 4 for
474 pointing out the need to test the effect of a much more intense saturating pulse.

475

476 **References**

477 Arnon DI, Whatley FR, Allen MB (1955) Vitamin K as a cofactor of photosynthetic
478 phosphorylation. *Biochimica et Biophysica Acta* **16**, 607-608

479 Asada K (2000) The water–water cycle as alternative photon and electron sinks.
480 *Philosophical Transactions of the Royal Society of London B: Biological Sciences*
481 **355**, 1419–1431

482 Edwards GE, Baker NR (1993) Can CO₂ assimilation in maize leaves be predicted
483 accurately from chlorophyll fluorescence analysis? *Photosynthesis Research* **37**,
484 89-102

485 Evans JR (2009) Potential errors in electron transport rates calculated from
486 chlorophyll fluorescence as revealed by a multilayer model. *Plant & Cell*
487 *Physiology* **50**, 698-706

488 Evans JR, Morgan PB, von Caemmerer S (2017) Light quality affects chloroplast
489 electron transport rates estimated from Chl fluorescence measurements. *Plant &*
490 *Cell Physiology* **58**, 1652-1660

491 Fan, DY, Fitzpatrick D, Oguchi R, Ma W, Kou J and Chow WS (2016) Obstacles in
492 the quantification of the cyclic electron flux around Photosystem I in leaves of C3
493 plants. *Photosynthesis Research* **129**, 239-251

494 Genty B, Briantais J-M, Baker NR (1989) The relationship between the quantum yield
495 of photosynthetic electron transport and quenching of chlorophyll fluorescence.
496 *Biochimica et Biophysica Acta* **990**, 87-92

497 Golding AJ, Finazzi G, Johnson GN (2004) Reduction of the thylakoid electron
498 transport chain by stromal reductants – evidence for activation of cyclic electron

- 499 transport upon dark adaptation or under drought. *Planta* **220**, 356-363
- 500 Klughammer C, Schreiber U (1994) An improved method, using saturating light
501 pulses, for the determination of photosystem I quantum yield via P700⁺-absorbance
502 changes at 830 nm. *Planta* **192**, 261-268
- 503 Klughammer C, Schreiber U (2007) Saturation Pulse method for assessment of energy
504 conversion in PS I. http://www.walz.com/e_journal/pdfs/PAN07002.pdf
- 505 Kohzuma K, Cruz JA, Akashi K, Hoshiyasu S, Munekage YN, Yokota A, Kramer DM
506 (2009) The long-term responses of the photosynthetic proton circuit to drought.
507 *Plant Cell and Environment* **32**, 209-219
- 508 Kou J, Takahashi S, Oguchi R, Fan D-Y, Badger MR, Chow WS (2013) Estimation of
509 the steady-state cyclic electron flux in white light, CO₂-enriched air and other
510 varied conditions. *Functional Plant Biology* **40**, 1018-1028
- 511 Kou J, Takahashi S, Fan D-Y, Badger MR, Chow WS (2015) Partially dissecting the
512 steady-state electron fluxes in Photosystem I in wild-type and *pgr5* and *ndh*
513 mutants of *Arabidopsis*. *Frontiers in Plant Science* **6**, Article 758
-
- 514 Miyake C (2010) Alternative electron flows (water-water cycle and cyclic electron
515 flow around PS I) in photosynthesis: molecular mechanisms and physiological
516 functions. *Plant and Cell Physiology* **51**, 1951-1963
- 517 Oguchi R, Douwstra P, Fujita T, Chow WS, Terashima I (2011) Intra-leaf gradients of
518 photoinhibition induced by different color lights: Implications for the dual

519 mechanisms of photoinhibition and for the application of conventional chlorophyll
520 fluorometers. *New Phytologist* **191**, 146–159

521 Öquist G, Chow, WS (1992) On the relationship between the quantum yield of
522 Photosystem II electron transport, as determined by chlorophyll fluorescence and
523 the quantum yield of CO₂-dependent O₂ evolution. *Photosynthesis Research* **33**,
524 51-62

525 Oxborough K, Baker NR (1997) Resolving chlorophyll *a* fluorescence images of
526 photosynthetic efficiency into photochemical and non-photochemical
527 components-calculation of qP and F_v'/F_m' without measuring F_o' . *Photosynthesis*
528 *Research* **54**, 135–142

529 Seaton GGR, Walker DA (1990) Chlorophyll fluorescence as a measure of
530 photosynthetic carbon assimilation. *Proceedings of the Royal Society of London B:*
531 *Biological Sciences* **242**, 29-35

532 Shikanai T (2007) Cyclic electron transport around photosystem I: genetic approaches.
533 *Annual Review of Plant Biology* **58**, 199-217

534 Terashima I, Fujita T, Inoue T, Chow WS, Oguchi R (2009) Green light drives leaf
535 photosynthesis more efficiently than red light in strong white light: Revisiting the
536 enigmatic question of why leaves are green. *Plant and Cell Physiology* **50**,
537 684-697

538 Weis E, Berry JA (1987) Quantum efficiency of Photosystem II in relation to

539 'energy'-dependent quenching of chlorophyll fluorescence. *Biochimica et*
540 *Biophysica Acta* **894**, 198-208

541 Yao H-S, Zhang, Y-L, Yi X-P, Zhang X-J, Fan D-Y, Chow WS, Zhang, W-F (2018)
542 Diaheliotropic leaf movement enhances leaf photosynthetic capacity and
543 photosynthetic use efficiency of light and photosynthetic nitrogen via optimizing
544 nitrogen partitioning among photosynthetic components in cotton (*Gossypium*
545 *hirsutum* L.). *Plant Biology*. DOI: 10.1111/plb.12678

546 Yi X-P, Zhang Y-L, Yao H-S, Han J-M, Chow WS, Fan D-Y, Zhang W-F (2018)
547 Changes in activities of both photosystems and the regulatory effect of cyclic
548 electron flow in field-grown cotton (*Gossypium hirsutum* L) under water deficit.
549 *Journal of Plant Physiology* **220**, 74-82

550

551

552

553 **Table 1. Estimate of the fraction of absorbed light partitioned to PS II (f_{II}) in leaf**
 554 **discs in 1% CO₂.** The average irradiance of modulated excitation was 0.05 $\mu\text{mol m}^{-2}$
 555 s^{-1} for blue or red excitation, and varied for green excitation (average irradiance in
 556 parentheses)

Spinach			Excitation light				
Actinic irradiance	blue	red	Green (0.05)	Green (0.07)	Green (0.18)	Green (0.38)	Average
16	0.47	0.48	0.52	-	-	0.47	
38	0.46	0.47	0.52	-	-	0.51	
81	0.49	0.49	0.53	-	-	0.49	
163	0.53	0.50	0.54	-	-	0.50	
506	0.53	0.51	0.52	-	-	0.51	0.50±0.02 (sd)

557

Poplar			Excitation light				
Actinic irradiance	blue	red	Green (0.05)	Green (0.07)	Green (0.18)	Green (0.38)	Average
13	0.54	0.43	-	0.39	-	0.54	
33	0.47	0.43	-	0.37	-	0.53	
72	0.48	0.42	-	0.44	-	0.52	
145	0.50	0.52	-	0.47	-	0.52	0.47±0.05 (sd)

558

Rice			Excitation light				
Actinic irradiance	blue	red	Green (0.05)	Green (0.07)	Green (0.18)	Green (0.38)	Average
20	0.46	0.49	-	0.43	0.53	0.44	
41	0.54	0.51	-	0.49	0.47	0.53	
84	0.52	0.51	-	0.50	0.50	0.56	
169	0.51	0.49	-	0.50	0.48	0.52	
523	0.60	0.52	-	0.49	0.46	0.50	0.50±0.04 (sd)

559

Cotton			Excitation light				
Actinic irradiance	blue	red	Green (0.05)	Green (0.07)	Green (0.18)	Green (0.38)	Average
16	0.46	0.45	-	0.43	-	0.35	
36	0.49	0.46	-	0.47	-	0.43	
76	0.49	0.49	-	0.48	-	0.45	
152	0.51	0.51	-	0.50	-	0.49	0.47±0.04 (sd)

560

561

562

563

564

565 **Table 2**

566

567 **The difference between ETR_1 and LEF_n ($\Delta Flux$) in spinach leaf discs, as affected**
 568 **by an inhibitor of cyclic electron transport or a mediator of oxygen reduction**

569

570 Leaf discs were vacuum infiltrated with water (control), 200 μM AA or 100 μM MV)
 571 and, after evaporation of excess intercellular water, were illuminated at two
 572 irradiances. Values are means for 3 to 4 leaf discs \pm s.d.

573

574

Treatment	$\Delta flux$	
	500 $\mu mol m^{-2} s^{-1}$	1000 $\mu mol m^{-2} s^{-1}$
water control	25.6 \pm 4.6	77.9 \pm 23.5
AA	2.3 \pm 13.6	-3.4 \pm 12.7
MV	0.3 \pm 5.8	-10.4 \pm 5.5

575

576

577

578

579

580 **Figure legends**

581 **Fig. 1.** Response of the linear photosynthetic electron flux of spinach leaf discs in 1%
582 CO₂ to the irradiance of actinic light from a halogen lamp. The linear electron flux
583 was measured either as the gross rate of oxygen evolution multiplied by 4 (●) or Chl
584 fluorescence excited by modulated light from light-emitting diodes emitting at blue
585 (◆, 0.05 μmol m⁻² s⁻¹), red (■, 0.05 μmol m⁻² s⁻¹) or green wavelengths (△, 0.05
586 μmol m⁻² s⁻¹; ▲, 0.38 μmol m⁻² s⁻¹). Values are means of six to seven leaf discs (±
587 s.d.).

588 **Fig. 2.** Response of the linear photosynthetic electron flux of poplar leaf discs in 1%
589 CO₂ to the irradiance of actinic light from a halogen lamp. The linear electron flux
590 was measured either as the gross rate of oxygen evolution multiplied by 4 (●, first
591 batch of plants; ○, second batch of plants) or Chl fluorescence excited by modulated
592 light from light-emitting diodes emitting at blue (◆, 0.05 μmol m⁻² s⁻¹), red (■, 0.05
593 μmol m⁻² s⁻¹) or green wavelengths (△, 0.07 μmol m⁻² s⁻¹, first batch of plants; ▲,
594 0.38 μmol m⁻² s⁻¹, second batch of plants). Values are means of nine to ten leaf
595 discs (± s.d.).

596 **Fig. 3.** Response of the linear photosynthetic electron flux of rice leaf segments in 1%
597 CO₂ to the irradiance of actinic light from a halogen lamp. The linear electron flux
598 was measured either as the gross rate of oxygen evolution multiplied by 4 (●) or Chl
599 fluorescence excited by modulated light from light-emitting diodes emitting at green

600 wavelengths (Δ , $0.07 \mu\text{mol m}^{-2} \text{s}^{-1}$; \diamond , $0.18 \mu\text{mol m}^{-2} \text{s}^{-1}$; \blacktriangle , $0.38 \mu\text{mol m}^{-2} \text{s}^{-1}$).

601 Values are means of five to six leaf discs (\pm s.d.).

602 **Fig. 4.** Response of the linear photosynthetic electron flux of cotton leaf discs in 1%

603 CO_2 to the irradiance of actinic light from a halogen lamp. The linear electron flux

604 was measured either as the gross rate of oxygen evolution multiplied by 4 (\bullet) or Chl

605 fluorescence excited by modulated light from light-emitting diodes emitting at blue

606 (\blacklozenge , $0.05 \mu\text{mol m}^{-2} \text{s}^{-1}$), red (\blacksquare , $0.05 \mu\text{mol m}^{-2} \text{s}^{-1}$) or green wavelengths (Δ , 0.07

607 $\mu\text{mol m}^{-2} \text{s}^{-1}$; \blacktriangle , $0.38 \mu\text{mol m}^{-2} \text{s}^{-1}$). Values are means of six leaf discs (\pm s.d.).

608 **Fig. 5.** Response of the total photosynthetic electron flux through PSI, ETR1 (\blacksquare)

609 and the Chl fluorescence-based linear photosynthetic electron flux through both

610 photosystems, LEF_{fl} (\bullet) of spinach leaves attached to the plant in air (a) or leaf discs

611 in 1% CO_2 (b). The difference between ETR1 and LEF_{fl} is ΔFlux (\blacktriangle), used as an

612 estimate of the cyclic electron flux around PSI. Values are means of seven leaves (\pm

613 s.d.).

614 **Fig. 6.** Response of the total photosynthetic electron flux through PSI, ETR1 (\blacksquare)

615 and the Chl fluorescence-based linear photosynthetic electron flux through both

616 photosystems, LEF_{fl} (\bullet) of poplar leaves attached to a branch of the plant in air (a) or

617 of leaf discs in 1% CO_2 (b). The difference between ETR1 and LEF_{fl} is ΔFlux (\blacktriangle),

618 used as an estimate of the cyclic electron flux around PSI. Values are means of

619 seven leaves (\pm s.d.).

620 **Fig. 7.** Response of the total photosynthetic electron flux through PSI, ETR1 (\blacksquare)

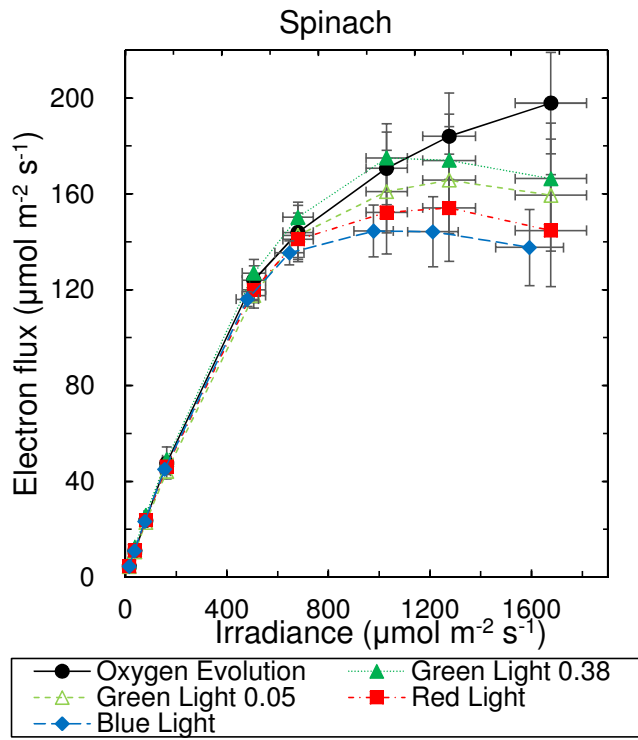
621 and the Chl fluorescence-based linear photosynthetic electron flux through both
622 photosystems, LEF_{fl} (●) of rice leaves attached to the plant in air (a) or of leaf
623 segments in 1% CO_2 (b). The difference between ETR1 and LEF_{fl} is $\Delta Flux$ (▲),
624 used as an estimate of the cyclic electron flux around PSI. Values are means of
625 seven leaves (\pm s.d.).

626 **Fig. 8.** Response of the total photosynthetic electron flux through PSI, ETR1 (■)
627 and the Chl fluorescence-based linear photosynthetic electron flux through both
628 photosystems, LEF_{fl} (●) of cotton leaves attached to the plant in air (a) or of leaf discs
629 in 1% CO_2 (b). The difference between ETR1 and LEF_{fl} is $\Delta Flux$ (▲), used as an
630 estimate of the cyclic electron flux around PSI. Values are means of seven leaves (\pm
631 s.d.).

632 **Fig. 9.** A plot of $qP \times I$ (a) and $F_v'/F_m' \times I$ (b) against irradiance I for cotton leaf
633 discs in 1% CO_2 . Values are means of nine leaves (\pm s.d.).

634

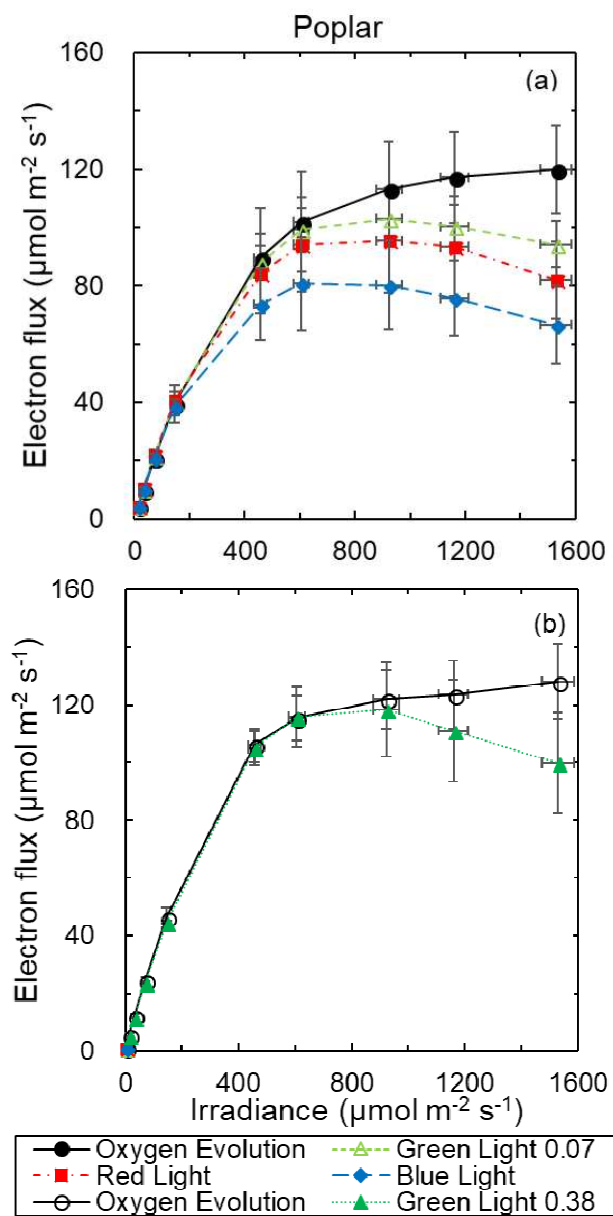
635 **Fig. 1**
636
637



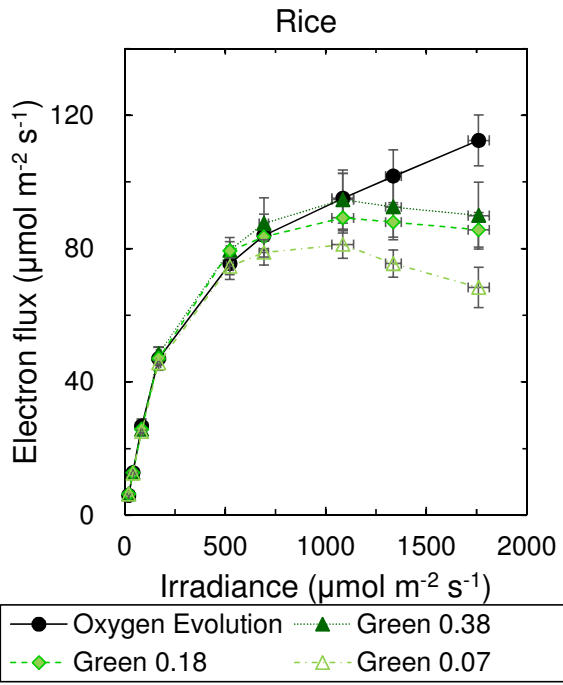
638
639
640

641 **Fig. 2**

642
643
644
645
646
647
648
649
650
651
652
653
654
655
656
657
658
659
660
661

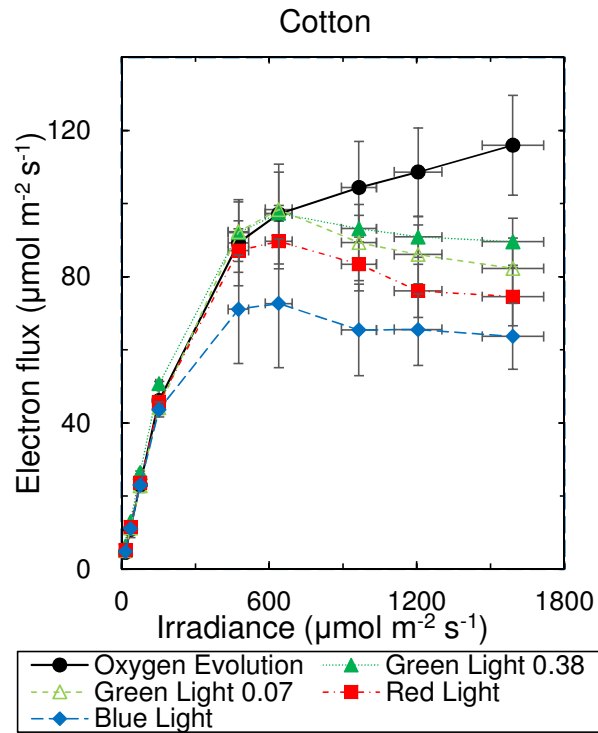


662 **Fig. 3**
663



664
665
666
667

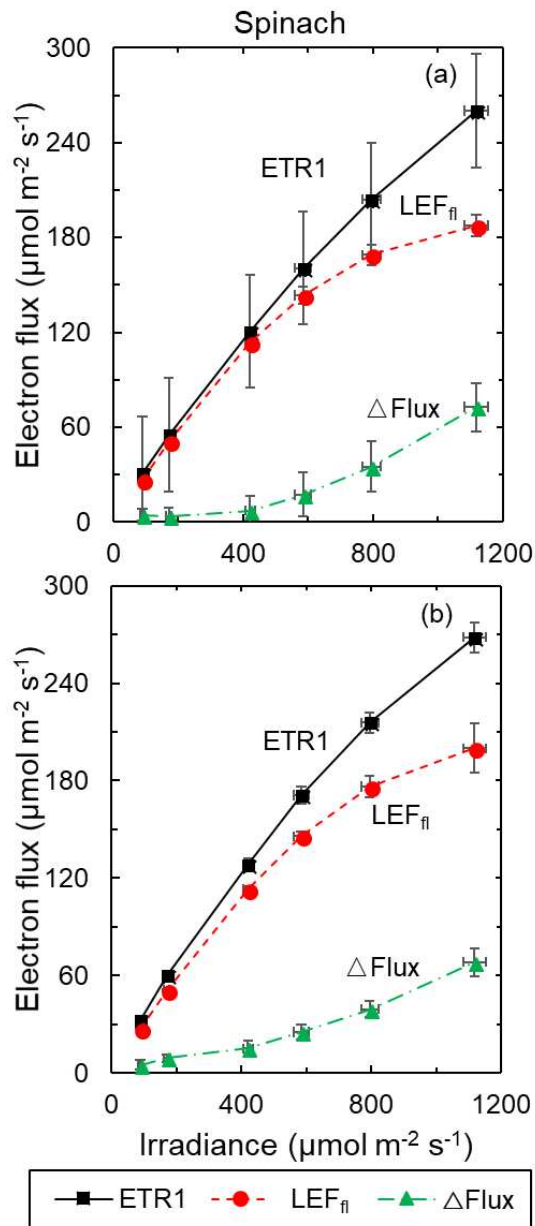
668 **Fig. 4**
669
670
671
672



673
674
675
676

677 **Fig. 5**

678
679
680
681
682
683
684
685
686
687
688
689
690
691
692
693
694
695
696
697
698
699
700
701
702
703
704
705
706
707
708
709
710
711
712
713
714
715
716
717
718
719



720
721
722
723
724
725
726
727
728
729
730
731
732
733
734
735
736
737
738
739
740
741
742
743
744
745
746
747
748
749
750
751
752
753
754
755
756
757
758
759
760
761
762

Fig. 6

Comment [张1]: Modify the graph

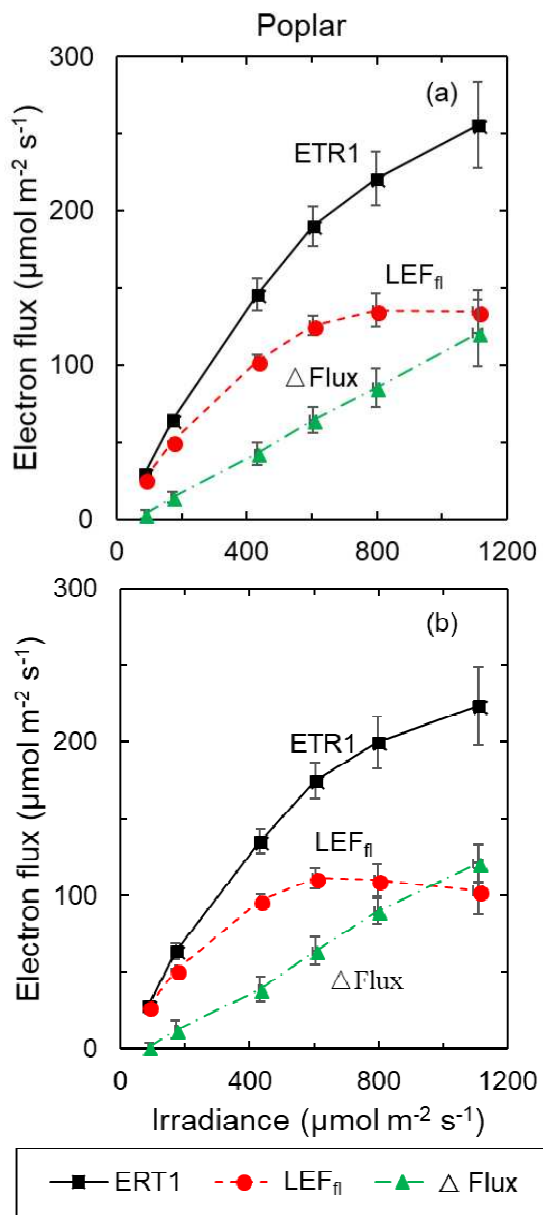
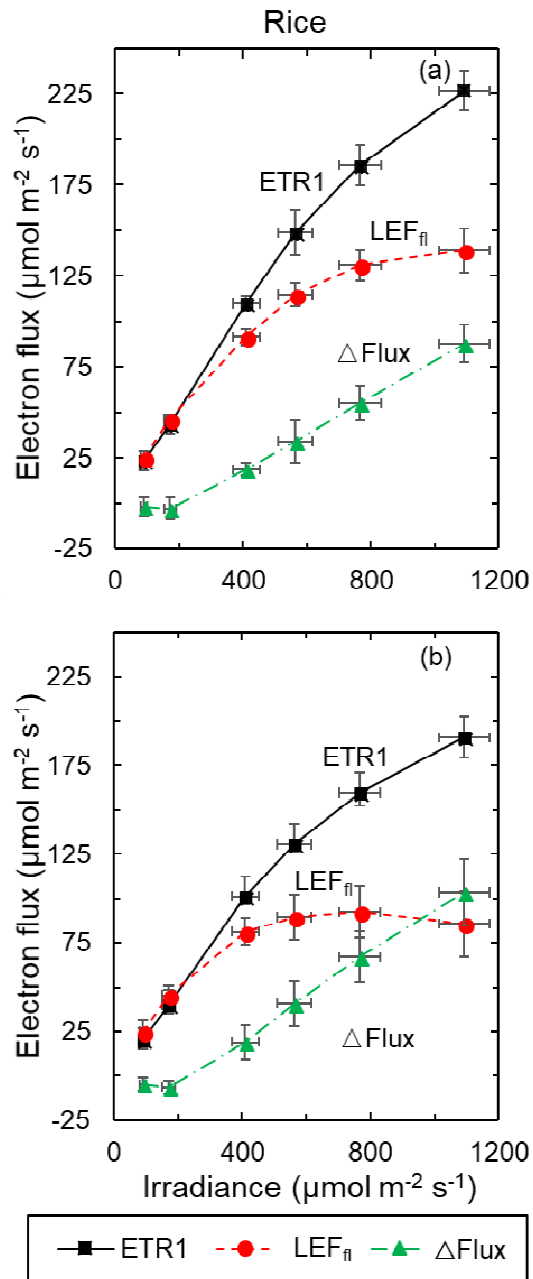
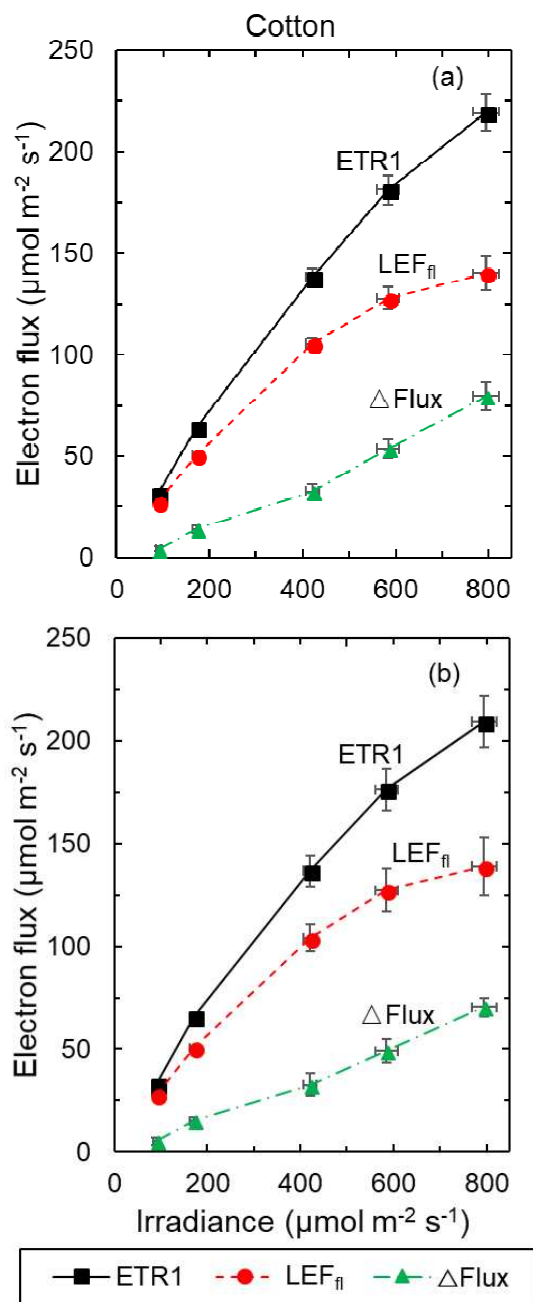


Fig. 7



807 **Fig. 8**

808
809
810
811
812
813
814
815
816
817
818
819
820
821
822
823
824
825
826
827
828
829
830
831
832
833
834
835
836
837
838
839
840
841
842
843
844
845
846
847
848
849
850



851 **Fig. 9**

852

853

854

855

856

857

858

859

860

861

862

863

864

865

866

867

868

869

870

871

872

873

874

875

876

877

878

879

880

881

